Catalysis Today 324 (2019) 15–26

Contents lists available at ScienceDirect

Catalysis Today

journal homepage: www.elsevier.com/locate/cattod

A review on dry reforming of methane in aspect of catalytic properties

Won-Jun Jang, Jae-Oh Shim, Hak-Min Kim, Seong-Yeun Yoo, Hyun-Seog Roh*

Department of Environmental Engineering, Yonsei University, 1 Yonseidae-gil, Wonju, Gangwon, 26493, Republic of Korea

ARTICLE INFO

Keywords:
Greenhouse gas
CO_2 utilization
Dry reforming of methane
Catalytic property
Sintering
Carbon formation

ABSTRACT

Because the whole world is under threat from climate change, 195 countries decided to reduce greenhouse gas (GHG) emissions by adopting the "Paris Agreement". The mitigation and utilization of GHG have become the most significant challenges in the area of green energy research. One feasible solution is the reforming of methane with carbon dioxide (called dry reforming of methane, DRM) that converts the two main GHGs (CO_2 and CH_4) into synthesis gas (H_2 and CO), which is a resource for the manufacture of useful value-added products. The main issue that needs to be addressed for DRM is the deactivation of catalysts by sintering and carbon formation. Design of a viable catalyst that exhibits high catalytic activity and stability, as well as resistance against deactivation, could be accomplished by making appropriate choices of active metal, support, promoter, structure and methods for preparation and activation. Numerous studies and reviews have dealt with various aspects of DRM. This review focuses on the physicochemical properties of the pertinent catalysts and their role in the catalytic performance needed for DRM. Specifically, the interaction between components, dispersion, particle size, basicity, oxygen storage capacity, reducibility, porosity and surface area are discussed. This study provides the understanding of catalytic properties and their correlation with catalytic performance needed for the rational design of catalysts and suitable for DRM.

1. Introduction

In December 2015, the Paris Agreement was adopted by 195 countries under the United Nations Framework Convention on Climate Change (UNFCCC) in order to cope with climate change [1,2]. The aim of the Paris Agreement was to restrict the rise of the global average temperature well below 2 °C above pre-industrial levels and to pursue efforts to limit the temperature increase even further to 1.5 °C by 2100 [1]. This international agreement for reducing greenhouse gas (GHG) emissions implies drastic alterations of the energy sector. To accomplish this ambitious goal, efficient, sustainable and integrated approaches are emerging as the energy sector on the verge of transformation, driven by technological progress such as electrification, decarbonization, sustainable energy resources and CO_2 capture and storage (CCS) and utilization (CCU) [3].

Carbon dioxide (CO_2), one of the GHGs, is a major contributor to the greenhouse effect, but it is also a natural source of carbon [4,5]. This offers several routes to generate useful fuels and chemicals while contributing to the reduction of CO_2 emission [3]. Recently, CH_4 has become a preferred energy resource, because of the discovery of abundant shale gas reserves and enhanced fracking technologies [6,7]. Apart from the shale gas reserves, biogas and landfill gas produced from anaerobic decomposition are also a significant source of CO_2 and CH_4 [8]. These conditions provided strong motivation for the dry reforming of methane [9,10]. It converts CO_2 and CH_4 into synthesis gas (H_2 + CO) with a H_2/CO ratio of 1.0 [11]. DRM not only utilizes CO_2 and CH_4 to reduce the emission of GHG, but also produces an industrially important synthesis gas, which is a resource for the manufacture of useful value-added products [12,13]. The synthesis gas with a H_2/CO ratio of 1.0 produced by DRM can be used for the synthesis of long chain hydrocarbons or oxygenate chemicals such as acetic acid, dimethyl ether and oxo-alcohols [14,15]. In addition, the H_2/CO ratio could be adjusted by converting CO with H_2O to CO_2 and H_2 in an additional water-gas shift step to the desired H_2/CO value of 2.0 for methanol and Fischer-Tropsch synthesis [16].

DRM is not regarded as an industrially mature process, despite of its apparent economic and environmental benefits [17]. The major obstacle preventing the commercialization of DRM is that carbon formation and sintering quickly deactivates conventional reforming catalysts [18,19]. In fact, only a few studies have dealt with the experimental application on industrial-scale DRM. Mortensen et al. (Haldor Topsøe) reported the use of traditional Ni catalysts at industrial-scale of DRM up to 133,000 $Nm^3\,h^{-1}$ required a co-feed of large amounts of steam in order to eliminate severe carbon formations [20]. Noble metal-based,

* Corresponding author.
E-mail address: hsroh@yonsei.ac.kr (H.-S. Roh).

https://doi.org/10.1016/j.cattod.2018.07.032
Received 31 March 2018; Received in revised form 24 June 2018; Accepted 13 July 2018
Available online 19 July 2018
0920-5861/ © 2018 Elsevier B.V. All rights reserved.

partly sulfur passivated Ni and Noble metal-promoted Ni catalysts had good potential for successful application of full-scale reforming plants, where only small amounts of steam were needed as co-feed. Therefore, a research on the DRM catalyst must be continued and intensified. A number of researchers have been intensively devoted to studying highly active and stable catalysts for DRM. Among the various types of catalysts that have been extensively studied for DRM are such as noble metals, transition metals, supported catalysts, spinel, perovskite and mesoporous catalysts [16–28]. In fact, these studies have succeeded in improving catalytic performance. In addition, several researchers have previously reported reviews of DRM that dealt with thermodynamics, kinetics, mechanisms, reactors and catalysts [16–28]. Typically, the catalysts reviewed were classified according to the kind of active metal, support, promoter and preparation method used with them [16–28]. Because recent catalysts are composed of a variety of components and utilize their intrinsic nature, a significant challenge when studying DRM is to interpret their complicated performance, characteristics and behavior.

This review discusses in detail the catalysts used for DRM, with particular attention paid to the role of their intrinsic nature in enhancing catalytic performance and in preventing deactivation. The significant role of interaction between components, dispersion, particle size, basicity, oxygen storage capacity, reducibility, porosity and surface area are reviewed. The aim of this work is to give a better understanding of key factors that should be taken into consideration in the design of pertinent catalysts.

2. Overview

2.1. Brief history

DRM was investigated as early as 1888 [29]. Fischer and Tropsch thoroughly studied the DRM reaction over Ni and Co catalysts in 1928 [30] and found severe carbon formation. Reitmeier et al. studied the combined H_2O and CO_2 reforming of hydrocarbon to moderate the carbon formation in 1949 [31]. They found a relationship between reactant composition and carbon formation [31]. Rostrup-Nielsen first tried to study extensively the catalysts for the reforming of hydrocarbons in 1964, particularly an intimate mixture of oxides of magnesium, aluminum, and nickel [32]. The preparation of these mixed oxides involved conversion of alumina and prat of the magnesia into spinel, whereas remaining magnesia during reforming acted as promoter to counteract carbon deposition.

In other and numerous data and studies, it was reported in the early 1990s that human activities were the dominant cause of the observed global warming, and in particular, that the most important reason was the emission of GHGs [33–35]. In addition to its potential role in managing GHGs, DRM is also attractive as a response to repeated oil crisis owing to its higher CO selectivity and low H_2/CO ratio, which are suitable for the synthesis of long chain hydrocarbons or oxygenate chemicals such as acetic acid, dimethyl ether and oxo-alcohols [36]. Since then, DRM has received renewed interest by utilizing the two major GHGs and a variety of catalysts for DRM have been widely tested [37]. DRM was tested over a number of catalysts based on the noble and non-noble metals [21]. Noble metals (Ir, Rh, Ru, Pt and Pd) have found to be much more resistance to inevitable carbon formation, but they are generally uneconomical [16]. Thus, noble metals can be used to decorate cheaper non-noble metals (Ni, Co) as a promoter, which helps to increase the dispersion, provide the additional active sites and improve their resistance to carbon formation [20]. Many researchers also investigated the influence of support, which determines not only the dispersion of active metal, but also its resistance against deactivation. The support could also possibly enhance catalytic activity while playing a significant role in the catalytic reaction [21]. In addition, there were many investigations of the promoters and methods of preparation and activation, in order to improve the performance of DRM catalysts [26].

2.2. Thermodynamics

DRM (Eq. (1)) is an extremely endothermic reaction.

$$CH_4 + CO_2 \rightarrow 2CO + 2H_2,\ \Delta H^0_{298} = 248\ kJ{\bullet}mol^{-1} \quad (1)$$

CH_4 and CO_2 are very stable molecules with high dissociation energy: 435 (CH_3-H) and 526 (CO-O) kJ mol^{-1}, respectively. Therefore, high temperatures are required to achieve the equilibrium conversion to synthesis gas. Moreover, the DRM reaction is more endothermic compared to the steam reforming (SRM, Eq. (2)) and autothermal reforming (ATR) of methane reactions. In the long term, therefore, supplying the required heat for the DRM reaction would have to use renewable energy sources for achieving sustainability purposes.

$$CH_4 + H_2O \rightarrow CO + 3H_2,\ \Delta H^0_{298} = 206\ kJ{\bullet}mol^{-1} \quad (2)$$

On the other hand, the equilibrium for the production of synthesis gas is generally influenced by the simultaneous occurrence of the reverse water gas shift (RWGS, Eq. (3)) reaction.

$$CO_2 + H_2 \rightarrow CO + H_2O,\ \Delta H^0_{298} = 41\ kJ{\bullet}mol^{-1} \quad (3)$$

This results in higher CO_2 conversion than that of CH_4 in equilibrium. In practice, this is advantageous for producing synthesis gas with a H_2/CO ratio of 1 or below 1 [36].

Apart from RWGS, the formation of carbon is the most important reason for fatal catalyst deactivation during DRM. As shown in Fig. 1, the carbon formed during DRM is primarily attributed to two reactions: (i) CH_4 decomposition (Eq. (4)) and (ii) Boudouard reaction (CO disproportionation, Eq. (5)) [38].

$$CH_4 \rightarrow C + 2H_2,\ \Delta H^0_{298} = 75\ kJ{\bullet}mol^{-1} \quad (4)$$

$$2CO \rightarrow C + CO_2,\ \Delta H^0_{298} = -172\ kJ{\bullet}mol^{-1} \quad (5)$$

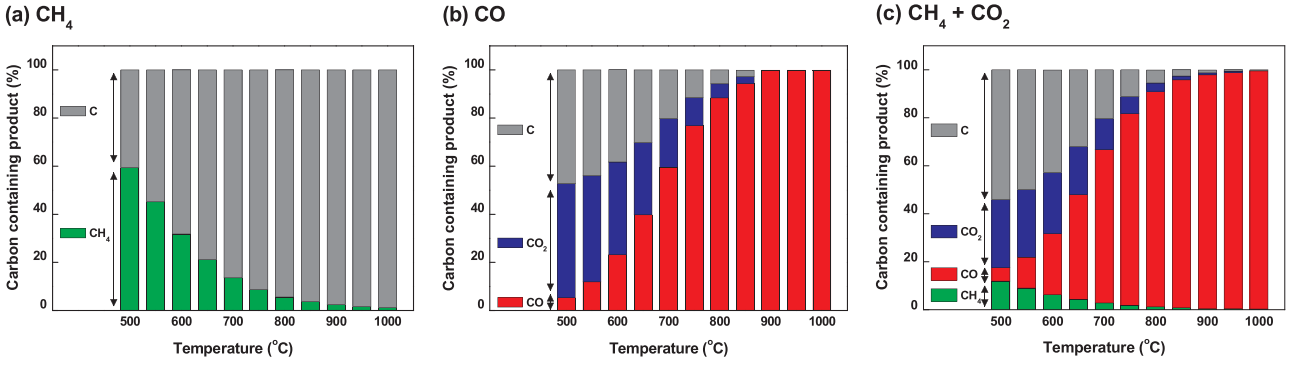

Fig. 1. Carbon containing product for the catalytic reactions: (a) CH_4 decomposition (CH_4 = 100%), (b) Boudouard reaction (CO = 100%), (c) Dry reforming of methane (CH_4 = 50% and CO2 = 50%). Adapted from Ref. [38]. Copyright 2016 Elsevier.

Wang et al. reported that CH_4 decomposition occurs above 557 °C, while the Boudouard reaction occurs below 700 °C [39]. They found that carbon is formed from CH_4 decomposition or the Boudouard reaction in the temperature range 557 to 700 °C and suggested that the optimum temperature at the feed ratio of CO_2/CH_4 = 1:1 is between 870 and 1040 °C, considering the conversion and carbon formation [39]. Several researchers have conducted thermodynamic simulations for various temperatures [21,38–41], CO_2/CH_4 ratios [41], pressures [38,39], additional oxidant [38,39] and consideration of various carbon formation reactions [41]. They commonly concluded that the operation of DRM at high temperatures above 850 °C and low pressures is required to attain high conversion [21,38–41]. Moreover, minimizing the yield of carbon formation is particularly essential to operate the DRM process stably [21,38–41]. However, it is difficult to generalize the formation of carbon by calculating thermodynamically the operation condition, because it is strongly dependent on the type of catalyst. Thus, DRM studies were conducted on the aspects of the catalysts.

2.3. Catalyst design

The development of highly active and stable catalysts with resistance against deactivation and economic feasibility is very important for successful industrialization of the DRM process. In general, active metals, supports, promoters, structure and methods for preparation and activation should be considered in designing an appropriate catalyst.

DRM has been investigated over supported metal catalysts based on noble (Rh, Ru, Pd, Pt and Ir) and non-noble (Ni and Co) metals. Noble metals were highly active for DRM with high resistance to carbon formation [37]. Ni- and Co-based catalysts were studied because of their cost effectiveness [42]. They showed activity comparable to that of noble metal-based catalysts, but they rapidly deactivated on account of either carbon formation or sintering. Thus, to date, both noble and non-noble metals have been used as active metals, and noble metals are utilized as a promoter in certain cases. Among these metals, Ni is the usual choice of active metal for commercialized steam reforming reactions at industrial scale [43].

In the first instance, the role of the support is literally to provide high surface area (SiO_2 and Al_2O_3) for the dispersion of the active metals. Furthermore, the stability of the support is very important in DRM because it operates at high temperatures. In addition to the conventional effect of the support, the support also plays an active role in the catalytic reaction. The support provides certain physicochemical properties such as basicity (CaO, La_2O_3 and MgO), oxygen storage capacity (CeO_2, CeO_2-ZrO_2 and TiO_2) and reducibility (CeO_2 and ZrO_2), which account for their intrinsic behavior in catalytic reactions, and also have implications for their resistance against carbon formation [44].

Promoters are classified as two types: textural (structural) and chemical (electronic) [23]. Textural promoters are typically utilized to avoid and delay the sintering of active species by enhancing the textural properties of the catalysts. Chemical promoters function to provide additional new active sites or to enhance the chemical property relating to the reactivity of the catalysts such as basicity or redox property. In particular, these chemical promoters help to moderate the formation of carbon and to oxidize carbonaceous species.

The preparation and activation methods used with catalysts strongly influence on their physicochemical properties and catalytic performance [45]. A suitable and proper preparation method gives better dispersion, stronger metal-support interaction and higher surface area. These are responsible for high activity, stability and resistance against sintering and carbon formation. In certain cases, an optimized preparation method strengthens the distinct ability of the support. In addition, the activation of catalysts has a significant role in the formation of active species, thereby influencing the catalytic performance.

Structured catalysts have particular potential for catalytic applications at high temperatures due to their well-dispersed active phase and high thermal stability [27]. Spinel (AB_2O_4, e.g. $MgAl_2O_4$) has been used as a support due to its superior stability at high temperatures. Perovskite (ABO_3, e.g. $LaNiO_3$) is well-known for having a high dispersion of active metal, as a result of the homogeneous solid solution of mixed oxides. Ordered mesoporous materials have shown their potential for application to DRM. The well-controlled nanoparticles can be obtained by embedding the active metals into the pores of the mesoporous materials (typically SiO_2).

3. Catalytic property and performance

The compositions in catalysts strongly affect their physicochemical properties, as discussed in Section 2.3. In particular, they influence the interaction between components, dispersion, particle size, basicity, oxygen storage capacity, reducibility, porosity and surface area, which are known for playing a significant role in the catalytic performance. The following section will discuss in detail various catalytic properties and their role in DRM.

3.1. Strong interaction

The interactions over the catalysts for DRM are typically classified as one of two kinds: (i) interaction between the active metal and support from the formation of a solid solution (i.e. cubic NiO-MgO, spinel ($NiAl_2O_4$ or $MgAl_2O_4$), perovskite ($LaNiO_3$, $La_{1-x}Sr_xNi_{0.4}Co_{0.6}O_3$, $La_{0.8}Sr_{0.2}Ni_{1-y}Co_yO_3$ and $BaZr_{(1-x)}Me_xO_3$) or (ii) interaction of bimetals from a synergetic effect. The strong metal support interaction (SMSI) is well-known for providing better active metal dispersion and resistance to sintering, which maintain the small size of the active species. This is typically responsible for strong resistance to carbon formation. The synergetic effect of bimetals helps to enhance dispersion as well as to provide additional active sites.

Ruckenstein and co-workers studied representatives of the strong metal-support interaction of catalysts for DRM [46]. They prepared Rh catalysts supported on reducible (CeO_2, Nb_2O_5, Ta_2O_5, TiO_2 and ZrO_2) and irreducible (γ-Al_2O_3, La_2O_3, MgO, SiO_2 and Y_2O_3) oxides. Rh/γ-Al_2O_3 and Rh/MgO showed high catalytic activity with stability among the irreducible supported catalysts. However, the Rh catalysts supported on SiO_2 and Y_2O_3 deactivated with time on stream. Their catalytic performance was attributed to the strong metal-support interaction, resulting from the formation of homogeneous solid solutions such as $MgRh_2O_4$, which was proposed on the basis of TPR and XRD. In the case of the reducible oxides, Nb_2O_5 showed a low activity, ZrO_2 and CeO_2 needed a long activation period, and Ta_2O_3 and TiO_2 rapidly deactivated. Authors concluded that the MgO and γ-Al_2O_3 were the most promising support for obtaining the best performance of Rh metal. They also tried to develop a non-noble catalyst strengthened by the strong metal-support interaction and focused on the NiO-MgO binary catalytic system [22,47–51]. Because the carbon is deposited on the active metal cluster when it is greater than a critical size and on the acidic support, they focused on these two factors for the design of anti-carbon formation: (i) controlling the size of the active metal cluster, (ii) the basicity of the support. MgO (4.2112 Å) is one of the basic alkaline earth metal oxides with a lattice parameter similar to that of NiO (4.1684 Å). In fact, the NiO-MgO catalyst (13.1 wt%) had a small Ni crystallite size of 7.3 nm, but the catalyst should be reduced at 500 °C for a long time of 14 h because of its low reducibility. Nevertheless, NiO-MgO solid solution catalyst exhibited the highest CH_4 and CO_2 conversions with anti-carbon formation among the Ni catalysts supported on alkali earth metal oxides.

Batiot-Dupeyrat et al. first tested perovskite catalysts for DRM and found that $LaNiO_3$ perovskite was active for the target reaction [52–54]. They also proposed the mechanism of the $LaNiO_3$ perovskite that $LaNiO_3$ perovskite transformed into La_2O_3 and Ni° after pre-reduction, and then changed into $La_2O_2CO_3$ and Ni° during DRM. After that, several researchers tried to find an active and stable perovskite

formula for DRM. Valderrama et al. intensively studied perovskite-type catalysts with the solid solution $La_{1-x}Sr_xNi_{0.4}Co_{0.6}O_3$ and $La_{0.8}Sr_{0.2}Ni_{1-y}Co_yO_3$ [55–57]. Doping with Sr promoted formation of Ni° and Co° active species highly dispersed on the $La_2O_2CO_3$ and SrO matrix, resulting from the solid solution formation. These active species were responsible for high activity and avoided carbon formation. Lima et al. investigated $La_{1-x}Ce_xNiO_3$ perovskite with varying Ce contents [58]. $La_{0.95}Ce_{0.05}NiO_3$ catalyst exhibited the highest activity, which was attributed to the united action of the perovskite structure by providing well-dispersed Ni metal. In addition, it was observed that it was possible to insert only a small amount of Ce into the perovskite structure, due to its low solubility. Caprariis et al. tested ternary perovskite type oxides $BaZr_{(1-x)}Me_xO_3$ with Rh, Ru and Pt for DRM [59]. $BaZrO_3$ perovskite structure showed excellent thermal stability owing to its ideal cubic phase and low coefficient of thermal expansion.

Sahli et al. tried to study the strength of interaction between active metal and support for DRM [60]. They prepared Ni/Al_2O_3 catalysts with various Ni/Al ratio denoted as Al-S (excess of Al and lack of Ni), S (stoichiometric $NiAl_2O_4$ spinel) and Ni-S (excess of Ni and lack of Al). The characteristic results indicated that Al-S mainly possessed $NiAl_2O_4$ species, while Ni-S included a considerable amount of free NiO. This caused differences in performance depending on the reaction temperature. Ni-S exhibited better performance at low temperatures, but suffered from severe carbon formation. In contrast, Ni-S showed excellent performance with resistance to carbon formation, as a result of limiting the growth of Ni species in the $NiAl_2O_4$ spinel structure.

Guo et al. investigated the Ni catalysts supported on γ-Al_2O_3, MgO-γ-Al_2O_3 and $MgAl_2O_4$ for DRM [61]. Ni/γ-Al_2O_3 rapidly deactivated with time on stream. Ni/MgO-γ-Al_2O_3 was more stable than Ni/γ-Al_2O_3, but it slightly deactivated after 10 h. In contrast, $Ni/MgAl_2O_4$ exhibited stable catalytic performance without deactivation. The solid solution formation of $MgAl_2O_4$ spinel formed over $Ni/MgAl_2O_4$ effectively suppressed the phase transformation of Ni or NiO to $NiAl_2O_4$ inactive spinel. The strong interaction between Ni and $MgAl_2O_4$ led to strong resistance to sintering, in particular, and the Ni particle size only increased 10.4–11.8 nm after the DRM reaction.

Apart from the strong metal to support interaction, Dalai and co-workers focused on the synergetic effect of bimetallic catalysts [40,62]. CO chemisorption results indicated that the Ni-Co bimetallic catalyst had a greater metal dispersion than did those of monometallic Ni or Co catalysts. In addition, the formation of Ni-Co alloy on the catalyst surface was confirmed from the shift of Ni and Co binding energy, resulting from the near-distance interaction between the two metal atoms.

In our previous reports, the metal oxides (MgO, CaO and La_2O_3) were introduced as promoters of $Ni\text{-}Ce_{0.8}Zr_{0.2}O_2$ catalysts for DRM [63,64]. As shown in Fig. 2, the addition of MgO led to the significant shift of the reduction peak toward higher temperatures, which indicated the strength of the interaction between NiO and the support/promoter. This clearly improved the resistance against both Ni sintering and carbon formation, which were confirmed by comparison of catalysts before and after catalytic reaction. MgO-promoted $Ni\text{-}Ce_{0.8}Zr_{0.2}O_2$ catalyst exhibited equilibrium CH_4 and CO_2 conversions for 200 h without detectable deactivation (Fig. 3), which was attributed to the improved sintering and carbon resistance that resulted from strengthening of the interaction between components. The comparison of the catalysts with strong metal to support interaction and the relation between SMSI and size of metal for DRM are summarized in Table 1. The results indicate that the formation of solid solution by SMSI is effective to obtain highly dispersed or small size of metal particles.

3.2. Dispersion and size

Iglesia's and co-workers intensively studied the DRM with isotopic tracer and kinetics over Rh, Ir, Pt, Ru and Ni supported on ZrO_2, γ-Al_2O_3, CeO_2-ZrO_2 and MgO in order to identify the reversibility of

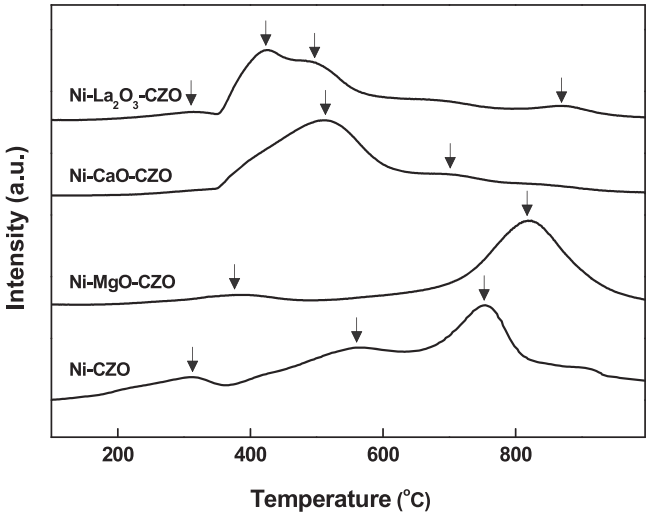

Fig. 2. TPR patterns of $Ni\text{-}Ce_{0.8}Zr_{0.2}O_2$ and metal oxide (MgO, CaO and La_2O_3) promoted $Ni\text{-}Ce_{0.8}Zr_{0.2}O_2$ catalysts. Adapted from Ref. [63]. Copyright 2015 Elsevier.

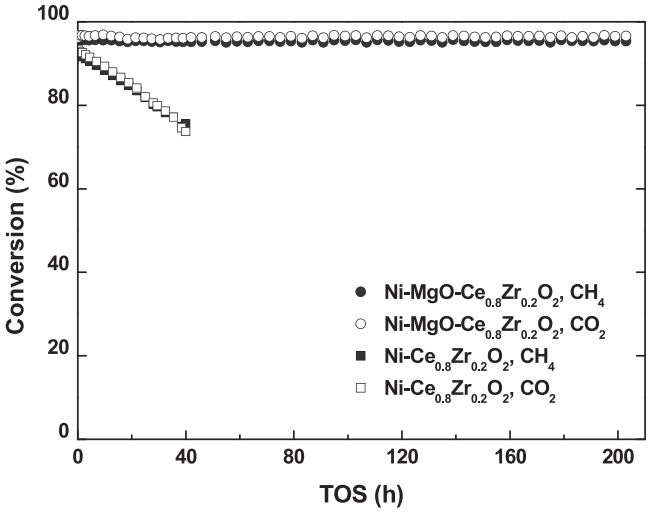

Fig. 3. Long-term stability of $Ni\text{-}Ce_{0.8}Zr_{0.2}O_2$ and $Ni\text{-}MgO\text{-}Ce_{0.8}Zr_{0.2}O_2$ catalyst for DRM (Reaction condition: T = 800 °C, CH_4:CO_2:N_2 = 1:1:3 and GHSV = 480,000 mL g_{cat}^{-1} h^{-1}). Adapted from Ref. [64]. Copyright 2013 Elsevier.

elementary steps and demonstrate the mechanism [65–70]. They reported that the turnover rate of CH_4 linearly increased with increasing CH_4 pressure, but it was not affected by CO_2, CO or H_2 pressure. These revealed that the surface of active species was not covered by CH_4-derived intermediates or products, because co-reactant or product pressures would have otherwise influenced forward turnover rates. They concluded that the activation of the C–H bond was the only kinetically relevant step in activation on the active metal cluster, and that the turnover rate of CH_4 on the active metal cluster increased with increasing dispersion. In addition, the rate of DRM was not affected by the chemical identity of the support, but the support significantly influenced only the dispersion and size of the active metal clusters.

Wang et al. tested the Ni catalysts supported on γ-Al_2O_3, CeO_2 and CeO_2-Al_2O_3 for DRM [71]. The catalytic activity of Ni/γ-Al_2O_3 was higher than that of Ni/CeO_2, but the high CH_4 conversion of Ni/γ-Al_2O_3 is due to the CH_4 decomposition, resulting in the catalyst deactivation by the carbon formation. Ni/CeO_2 showed the highest resistance against carbon formation owing to its highest Ni dispersion and oxidative properties of CeO_2. The optimal loading of CeO_2 promoter was

Table 1
Comparison of the catalysts with strong metal to support interaction in DRM.

Catalyst[a]	Reaction condition			Conversion (%)		Time on stream (h)	Characterization techniques	Remarks	Reference
	GHSV or Flow rate	Feed gas ratio	T (K)	CH_4	CO_2				
Rh, γ-Al_2O_3/MgO/La_2O_3, Imp	60,000 mL g_{cat}^{-1} h^{-1}	CH_4:CO_2 1:1	1073	82 80 68	87 86 78	50	XRD H_2-TPR	Strong metal-support interaction formed by $MgRh_2O_4$ improves dispersion and enhances the resistance against sintering (Rh surface area (m^2 g_{cat}^{-1} (×100)): MgO (41.8) > ZrO_2 (11.1) > TiO_2 (10.2) > CeO_2 (9.9))	[46]
Ni, MgO, Imp	60,000 mL g_{cat}^{-1} h^{-1}	CH_4:CO_2 1:1	1073	95	91	120	XRD H_2-TPR	The formation of NiO-MgO solid solution controls the size of Ni active species	[47,48,49,50,51]
Ni, $Ce_{0.8}Zr_{0.2}O_2$, MgO, CoP	480,000 h^{-1}	CH_4:CO_2:N_2 1:1:3	1073	95	96	200	H_2-TPR	The addition of MgO leads to the enhancement of the sintering and carbon resistance, resulting from the strong interaction between Ni and support/promoter (Ni crystallite size of fresh and used catalysts (nm): Ni-MgO-CZO (8.9 → 9.2) < Ni-CZO (8.4 → 12.8) < Ni-La_2O_3-CZO (8.5 → 15.3) Ni-CaO-CZO (9.3 → 16.4))	[63,64]
Co, La_2O_3, Sr, SG	24 L g_{cat}^{-1} h^{-1}	CH_4:CO_2 1:1	1073	94	99	30	XRD H_2-TPR SEM	Doping Sr promotes to form Ni^0 and Co^0 active species highly dispersed on the $La_2O_2CO_3$ and SrO matrix, resulting from the solid solution formation (Co particle size (nm): $La_{0.6}Sr_{0.4}CoO_3$ (10) < $La_{0.8}Sr_{0.2}CoO_3$ (12) < $LaCoO_3$ (15))	[57]
Ni-Co, MgO-Al_2O_3, CoP	11.7 L g_{cat}^{-1} h^{-1}	CH_4:CO_2:N_2 1:1:1	1023	84	87	28	H_2-TPR XPS	Ni-Co bimetal catalyst shows high catalytic activity, resulting from strong metal to support interaction	[40]

[a] Metal, Support, Promoter, Preparation method.

found to be 1 ± 5 wt%. CeO_2 promoters played a role in reducing the chemical interaction between Ni and γ-Al_2O_3, resulting in an increase in reducibility and stronger dispersion of Ni. In addition, the type of carbon formed on Ni/CeO_2 was carbonate species, which can be easily oxidized compared to the graphitic carbon formed on Ni/γ-Al_2O_3 and Ni/CeO_2-Al_2O_3. Likewise, Xu et al. studied the behavior of carbon formation on the Ni/Al_2O_3 catalysts promoted by MgO and CeO_2 in DRM [72]. Both MgO and CeO_2 promoters were effective at improving resistance against carbon formation in the catalytic reaction. They tried to investigate the characteristics of carbon formation and measured the temperature at the beginning (T_B) and end (T_E) of carbon formation from temperature programmed carbon deposition with different feed ratios of CO_2/CH_4. T_E of CeO_2-promoted catalysts were significantly lower than those of non-promoted catalysts. This was attributed to the role of CeO_2 in enhancing the Ni dispersion and facilitating electron transfer.

Črnivec et al. prepared Ni-Co bimetallic catalysts supported on CeO_2-ZrO_2 (80/20) with different preparation method of hydrothermal (HT) and glycothermal (EG) and various nickel and cobalt loading (3, 6, 12 and 18%) for DRM [73]. The catalysts containing active metal particles smaller than 6 nm exhibited superior resistance to carbon formation on the surface, but they showed certain activity for RWGS. The catalysts with large active metal particle sizes occurred the CH_4 dehydrogenation consequentially accumulated considerable amounts of carbon formation on their surface.

Xu et al. insisted on the importance of the amount of accessible Ni active centers and the size of Ni particles in DRM [74]. The ordered mesoporous framework of NiO-MgO-Al_2O_3 oxides played a significant role in providing accessible Ni active centers and in stabilizing Ni particles by the confinement effect. A moderate amount of Mg modifier offered advantageous properties. The catalyst with 2% Mg exhibited intense ability for avoiding carbon formation due to the fact that the effect of nano-sized Ni particles contributed to suppressing carbon formation. Likewise, Jun et al. also investigated Ni-MgO-Al_2O_3 catalysts with various Mg/Al ratios for DRM. Ni-Al_2O_3 showed poor activity and stability because of the formation of inactive $NiAl_2O_4$ spinel [75]. Ni-MgO showed stable activity, but its conversion was lower than that of Ni-MgO-Al_2O_3. The proper addition of Al_2O_3 to a MgO matrix led to better Ni dispersion, resulting from structural promotion by Al_2O_3 and improved exposure of Ni metal particles caused by replacing NiO with MgO in the spinel structure. Ni-MgO-Al_2O_3 catalyst with the MgO/(MgO + Al_2O_3) ratio of 0.44-0.86 showed higher conversion with stability than those of Ni-Al_2O_3 and Ni-MgO in DRM. Rezaie's and coworkers also pointed out that the well dispersed Ni particles supported on $MgAl_2O_4$ were the main reason for its excellent catalytic performance in DRM [76–80]. Rahemi et al. also emphasized the significance of dispersion and the size of active metals [81].

In our recent result (Fig. 4), we demonstrate that the turnover frequency strongly depends on the size of the Ni particles and that the overall conversion was affected by the number of Ni active sites. These are estimated from the reduction degree and Ni particle size, which are controlled by the strength of the Ni-support/promoter interaction [82]. Although Ni-MgO-$Ce_{0.6}Zr_{0.4}O_2$ possessed the highest oxygen storage capacity (OSC) among the prepared catalysts, Ni-MgO-$Ce_{0.8}Zr_{0.2}O_2$ catalyst showed the best performance because of its high degree of reduction and small Ni particle size. This study clarified the effect of Ni particle size on the catalytic performance at a fixed target temperature, and the dependence of Ni particle size on the nature of the support. The comparison of the catalysts with dispersion and size for DRM is summarized in Table 2.

3.3. Basicity

The formation of carbon from CH_4 decomposition is well-known to be formed on the acid sites of the support. Thus, basicity is a key property for determining the resistance against carbon formation in

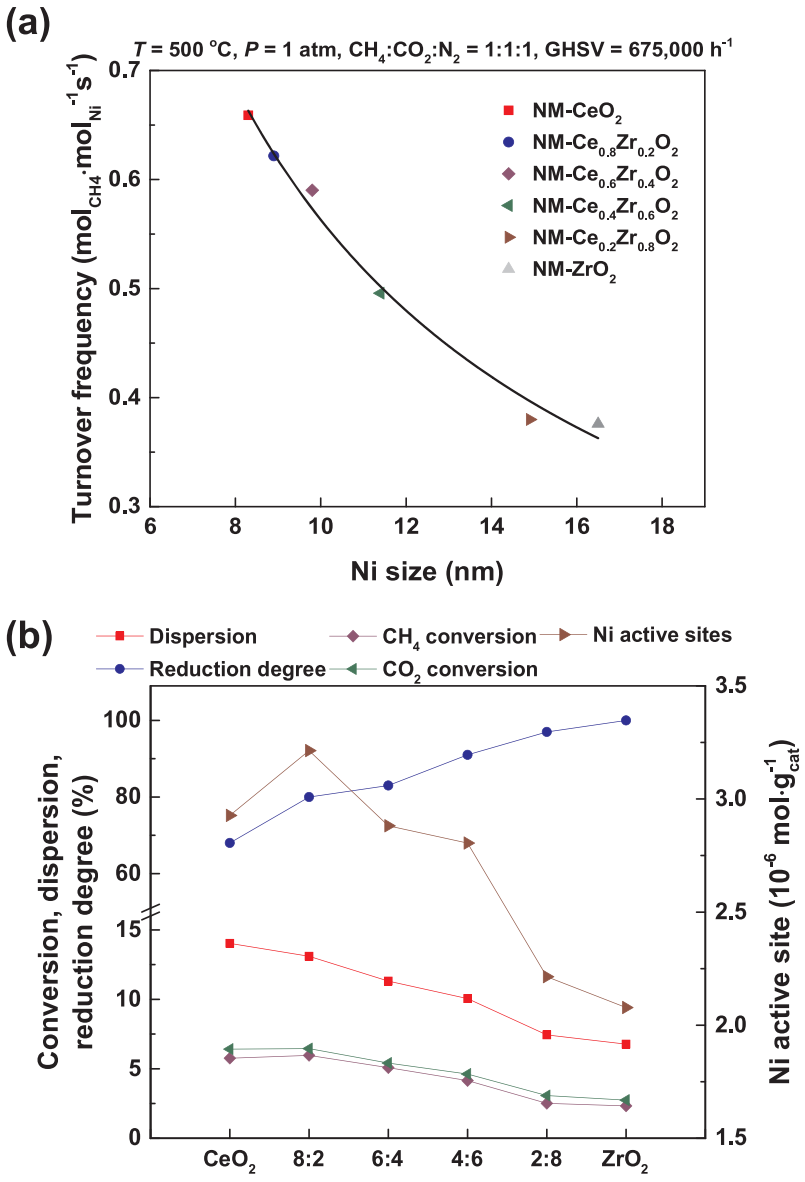

Fig. 4. Relation between physicochemical properties and DRM results (T = 500 °C, CH_4:CO_2:N_2 = 1:1:1 and GHSV = 675,000 mL g_{cat}^{-1} h^{-1}): (a) TOF vs. Ni particle size, (b) Conversion vs. Ni dispersion, reduction degree and metal active sites. Adapted from Ref. [82]. Copyright 2018 Royal Society of Chemistry.

DRM. Alkaline and alkaline earth metals are widely used as support or promoter. These metals decrease the acidity of the support and play the role of poison for active metals to some extent, which results in decreasing the rate of hydrocarbon cracking. In addition, increasing the basicity of the catalyst accelerates the activation of mildly acidic CO_2, that oxidizes the surface carbon [83–85]. The presence of activated CO_2 on the catalyst surface inhibits the carbon formed from the CH_4 decomposition reaction, resulting in improving the resistance to deactivation [86].

Park's and co-workers studied the alkaline-promoted zeolite supported Ni catalysts for DRM [87,88]. The addition of alkaline promoter (K and CaO) led to the favorable adsorption of CO_2 on the surface adjacent Ni sites to form carbonate species. This resulted in superior resistance against carbon formation, supplying surface oxygen from CO_2 adsorption, which was helpful in preventing the sequential build-up of surface carbon. Choudhary et al. tested NiO/CaO and Ni/Al_2O_3 catalysts precoated with MgO, CaO and rare-earth metals for DRM [89,90]. They reported the possibility of MgO-precoated Ni/Al_2O_3 catalyst, which showed the best catalytic performance. Likewise, Dias et al. also studied Ni/CaO/γ-Al_2O_3 catalysts with various CaO contents for DRM. They demonstrated that the addition of small amounts of CaO increased the CO_2 conversion by strongly attracting CO_2 gas to the catalyst surface [91]. Sengupta et al. investigated the effect of modifying the support with CaO or MgO to improve the catalytic activity of Al_2O_3 supported Ni and Ni-Co catalyst for DRM [92]. The modified-Al_2O_3 supported Ni and Ni-Co catalysts containing CaO showed additional basic sites, resulting in increased amounts of chemisorbed H_2 and CO_2. These sites were attributed to improved catalytic activity with resistance against carbon formation. The presence of MgO led to poor reducibility at 873 K owing to the strong interaction of MgO with Ni and Co. This resulted in the decrease of conversion apart from its basicity. The comparison of the catalysts with basicity for use in DRM is summarized in Table 3.

3.4. Oxygen storage capacity

In addition to the basicity of the support, one of important factor is the oxygen storage capacity that contribute to the activation of CO_2 [93]. The oxygen defects in supports are potential sites for the activation of CO_2 and cleavage of C–O bond, which increase the number of

Table 2
Comparison of the catalysts with dispersion and size in DRM.

Catalyst[a]	Reaction condition		Conversion (%)			Time on stream (h)	Characterization techniques	Remarks	Reference
	GHSV or Flow rate	Feed gas ratio	T (K)	CH_4	CO_2				
Ni, CeO_2, Al_2O_3, Imp	2,400 mL g_{cat}^{-1} min^{-1}	CH_4:CO_2 1:1	973	80	80	25	XRD	Ni/CeO_2 shows the highest resistance against carbon formation owing to its highest Ni dispersion	[71]
Ni-Co, $Ce_{(1-x)}Zr_{(x)}O_2$, EG	37 L g_{cat}^{-1} h^{-1} (WHSV)	CH_4:CO_2 1:1	1073	67	56	20	XRD H_2-Chem SEM	The catalysts containing active metal particles smaller than 6 nm exhibits superior resistance to carbon formation on the surface	[73]
Ni, Al_2O_3, MgO, CoP	15,000 mL g_{cat}^{-1} h^{-1}	CH_4:CO_2 1:1	1073	95	96	100	XRD	The introduction of proper amount of Mg controls Ni particle size, which contributes to suppressing the carbon formation	[74]
Ni. Al_2O_3, MgO, SG	36,000 mL g_{cat}^{-1} h^{-1}	CH_4:CO_2:N_2 1:1:1	1073	87	90	40	H_2-TPR TEM	The proper addition of Al_2O_3 into MgO matrix leads to better Ni dispersion, resulting from the structural promotion by Al_2O_3 and improved exposure of Ni metal particles caused by replacing NiO with MgO in spinel structure.	[75]
Ni, Al_2O_3-ZrO_2, Imp	24 L g_{cat}^{-1} h^{-1}	CH_4:CO_2 1:1	1123	98	98	24	XRD TEM	A high dispersion of Ni particles results in high activity in the CDR reaction	[81]
Ni, $Ce_{(1-x)}Zr_{(x)}O_2$, MgO, CoP	1,620,000 mL g_{cat}^{-1} h^{-1}	CH_4:CO_2:N_2 1:1:1	1073	74	85	5	XRD H_2-TPR XAS	The turnover frequency strongly depends on the size of the Ni particles and the overall conversion is affected by the number of Ni active sites, estimated from the reduction degree and Ni particle size, which are controlled by the strength of the Ni-support/promoter interaction	[82]

[a] Metal, Support, Promoter, Preparation method.

mobile oxygens on the catalyst surface. The mobile oxygens oxidize C to CO and form carbonate intermediate species on basic reducible supports, resulting in eliminating the carbon formation [94].

Lercher's and co-workers studied CO_2 activation on supported Pt catalysts in relation to DRM [95–98]. They proved that CH_4 activated on the active metal reacted with carbonate species activated from CO_2 on the support in the proximity of active metal particles. In addition, they emphasized the significant role of support by exhibiting the low activity results of Pt black and Pt/SiO_2, which were incapable of forming carbonates on the support. According to the reactivity results of coke formed on the Pt/Al_2O_3 and Pt/ZrO_2, the ability of CO_2 activation on the oxygen defect site of the ZrO_2 support was verified.

Park's and co-workers tried to apply the Ni catalysts supported on the ZrO_2 support for DRM [99–105]. A series of Ni/ZrO_2 catalysts with a wide range of Ni contents from 2.5 to 23% were tested for DRM. Ni/ZrO_2 catalysts with more than 10% Ni content formed a large amount of carbon, but the carbon acted as an intermediate to react with oxygen species from CO_2 decomposition. The removable property of the deposited carbon contributed to the stability of Ni/ZrO_2 in DRM. On the basis of this result, they prepared Ce-modified ZrO_2 support and intensively studied the role of the oxygen storage capacity in improving the catalytic performance for reforming reactions. Ni catalysts supported on CeO_2-ZrO_2 mixed oxides were first applied to the reforming of methane with O_2 or H_2O. In fact, the catalytic performance was significantly improved owing to the ability to make mobile oxygen species and better Ni dispersion.

Roh et al. tested Ni catalysts supported on CeO_2-ZrO_2 for DRM. The homogeneous CeO_2-ZrO_2 solid solution was successfully synthesized using co-precipitation method [106–109]. Cubic $Ni\text{-}Ce_{0.8}Zr_{0.2}O_2$ was more stable than $Ni\text{-}CeO_2$ and more active than $Ni\text{-}ZrO_2$. This was due to the enhanced oxygen storage capacity caused by the partial substitution of Ce^{4+} by Zr^{4+} and high Ni dispersion.

Wang et al. investigated Ir catalysts supported on CeO_2, $Ce_{0.9}Pr_{0.1}O_2$ and $Ce_{0.9}Zr_{0.1}O_2$ mixed oxides for DRM [110]. The doping of Pr or Zr into a CeO_2 matrix improved the oxygen storage capacity, resulting in rapid gasification of carbon formed at the metal-support boundary.

Zhu et al. prepared $Ni\text{-}Ce/SiO_2$ catalysts under various conditions of calcination and found that the calcination condition influenced the initial oxidation state of CeO_2 (Ce^{3+}/Ce^{4+}) [111]. The mobility and activity of surface oxygen on CeO_2 promoted the gasification of carbon. A comparison of the catalysts with oxygen storage capacity for DRM is summarized in Table 3.

3.5. Reducibility

The metallic state of transition and novel metals is typically considered as the active phase of DRM. Prior to the catalytic reaction, an activation step is required to reduce the initial oxide phases to the catalytically active metallic phase. The degree of reduction influences the number of available active sites. In certain cases, too strong interaction between active metals and supports caused poor reducibility or the formation of inactive phase, resulting in the lack of active sites. In fact, Gadalla and Bower pointed out that the formation of $NiAl_2O_4$ spinel in Al_2O_3 supported Ni catalysts led to the disintegration of the catalyst structure [36]. $NiAl_2O_4$ spinel stabilized Ni in the inactive divalent oxidation state (Ni^{2+}), which is hard to reduce.

Valentini et al. investigated the role of V doping of the Ni/Al_2O_3 catalyst in DRM [112]. V induced microstructural changes in the Ni metal on the Al_2O_3 support. Ni/Al_2O_3 catalyst presented the formation of nickel aluminate spinel ($NiAl_2O_4$), which is inactive for DRM. With the addition of V, $NiAl_2O_4$ formation was suppressed by maintaining Ni° and Al_2O_3 species, as a result of enhanced reducibility. V-doped Ni/Al_2O_3 catalyst showed better CH_4 and CO_2 conversions, but V content above 3.7% promoted carbon formation. Li et al. studied the effect on ZrO_2 addition in Ni/Al_2O_3 catalyst for DRM [113]. They found that the degree of reduction of NiO supported on Al_2O_3-ZrO_2 was above 0.9, which was clearly higher than that of NiO supported on Al_2O_3 (0.7). The introduction of ZrO_2 improved the reducibility of the catalysts as a result of the reducible nature of ZrO_2. Meanwhile, ZrO_2 helped to reduce NiO species to metallic Ni and avoided the formation of inactive $NiAl_2O_4$ simultaneously. This was a key factor for preventing carbon formation in DRM. Juan-Juan et al. and Luna et al. also noted the

Table 3
Comparison of the catalysts with basicity and oxygen storage capacity in DRM.

Catalyst[a]	Reaction condition		Conversion (%)			Time on stream (h)	Characterization techniques	Remarks	Reference
	GHSV or Flow rate	Feed gas ratio	T (K)	CH_4	CO_2				
Ni, K/Ca, Zeolite, hybridized by the solid-state method	60,000 h^{-1}	CH_4:CO_2:N_2 1:1:2.2	1073	90	90	140	FT-IR (Basicity)	The addition of alkaline promoter leads to the favorable adsorption of CO_2 on the surface adjacent Ni sites, resulting in the superior resistance against carbon formation	[87,88]
Ni-Co, Al_2O_3, CaO, IWI	0.14 kg_{cat} h kg_{CH4}^{-1}	CH_4:CO_2:N_2 1:1:3	873	15	21	3	CO_2-TPD H_2-TPD (Basicity)	Additional basic sites generated by the addition of CaO increase the amount of chemisorbed H_2 and CO_2	[92]
Ni, Al_2O_3, CeO_2, IWI	12,000 mL g_{cat}^{-1} h^{-1}	CH_4:CO_2 1:1	1073	85	92	100	XPS (OSC)	Calcination condition affects the initial state of CeO_2 (Ce^{3+}/Ce^{4+})	[111]
Pt, Pt black/Al_2O_3/ZrO_2/SiO_2	566 mL g_{cat}^{-1} min^{-1}	CO_2:CH_4:He:N_2 42:42:75:10	875		30	500	IR (OSC)	Existence of oxygen vacancy is important because CO_2 is activated on the oxygen vacancy sites of ZrO_2	[95,96,97,98]
Ni, ZrO_2	60,000 g s m^{-3}	CH_4:CO_2:N_2 1:1:3	1023	90	100	30	–	Deposited carbons on the catalysts easily react with mobile oxygen species of ZrO_2	[99,100,101,102,103,104,105]
Ni, $Ce_{0.8}Zr_{0.2}O_2$, CoP	216,000 mL g_{cat}^{-1} h^{-1}	CH_4:CO_2:N_2 1:1:1	1073	92	93	100	H_2-TPR (OSC)	The addition of Zr enhances the oxygen storage capacity of Ni-CeO_2 catalyst, resulting in high activity for DRM reaction	[106,107,108,109]

[a] Metal, Support, Promoter, Preparation method.

promotional effect of K on the reducibility of Ni/Al_2O_3 catalyst, which facilitated the reduction of Ni species which strongly interacted with Al_2O_3 support [114,115]. TPR results of K-promoted Ni/Al_2O_3 catalysts showed that K had an ability to retain Ni species as a free NiO which had relatively weak interaction with Al_2O_3 support.

Tomishige's and co-workers tested NiO-MgO solid solution catalyst for the reforming reaction, but this catalyst was hard to activate at the reaction temperature of 800 °C [116–118]. They found that the addition of a small amount of Pt (0.1%) led to decrease of the reduction temperature of H_2 pretreatment because of the high reducibility of Pt. They also reported the similar results that Pt-modified Ni/Al_2O_3 catalyst exhibited better catalytic performance than Pt/Al_2O_3 or Ni/Al_2O_3 for DRM owing to the enhancement of the catalyst reducibility via alloying and/or hydrogen spillover effect.

In our previous work, the preparation method (co-precipitation, co-impregnation and sequential impregnation) of MgO-promoted Ni-$Ce_{0.8}Zr_{0.2}O_2$ catalysts were systemically changed [119]. As shown in Fig. 5, TEM mapping results showed the formation of NiO-MgO or CeO_2-ZrO_2 solid solution on the impregnated catalysts. In the case of only co-precipitated catalyst, four elements (Ni, Mg, Ce and Zr) were located at the same position. This resulted in easier reducibility, which was confirmed from H_2-TPR. The co-precipitated catalysts showed stable catalytic performance without detectable deactivation for 200 h in DRM. The comparison of the catalysts with reducibility for DRM is summarized in Table 4.

3.6. Porosity and surface area

Mesoporous materials are used for various catalytic application, due to their high specific area, uniform and their interconnected porosity. Their unique properties were hard to maintain at high temperatures, but the recent development of synthesis technology has led to the application of these kinds of materials.

Liu et al. prepared a Ni-incorporated MCM-41 mesoporous molecular sieve with various Ni loadings [120]. The catalytic activity for DRM was closely proportional to the number of active species, estimated by H_2 chemisorption. The noticeable point was that Ni/MCM-41 was more stable than conventional Ni/SiO_2, as a result of the stabilized dispersion of active species by the silica matrix and/or the surrounding unreduced Ni ions. Moradi et al. reported that the ratio of Si/Al on Ni/ZSM-5 played a crucial role in creating the well-crystallized structure of nano-sized catalysts [121]. Xu et al. prepared the ordered mesoporous tricompound NiO-CaO-Al_2O_3 oxides [122]. These were synthesized via a facile one-pot evaporation-induced self-assembly strategy. The obtained mesoporous materials showed advantageous textural properties and superior thermal stabilities. In particular, this property played a significant role in providing more accessible Ni active centers and stabilizing the Ni nanoparticles by the confinement effect. The comparison of the catalysts with porosity and surface area for DRM is summarized in Table 5.

4. Conclusions and perspective

In the near future, the catalytic reforming of methane with carbon dioxide can be utilized for reducing greenhouse gas emissions and producing green chemicals and fuels, combining with a renewable and cost-effective source of electricity. The primary issues are carbon formation and sintering, which in turn leads to the deactivation of DRM catalysts. The catalytic performance and resistance against deactivation are affected by the active metal, support, promoter, structure and methods for preparation and activation. Because the effects of their behavior on the performance of catalysts are usually complex, catalyst designers face a tradeoff between merits and demerits. In this review, we discussed the influence of various catalytic properties on the target reaction in order to provide a guideline for designing an appropriate catalyst. First of all, the SMSI is the one of most important property for

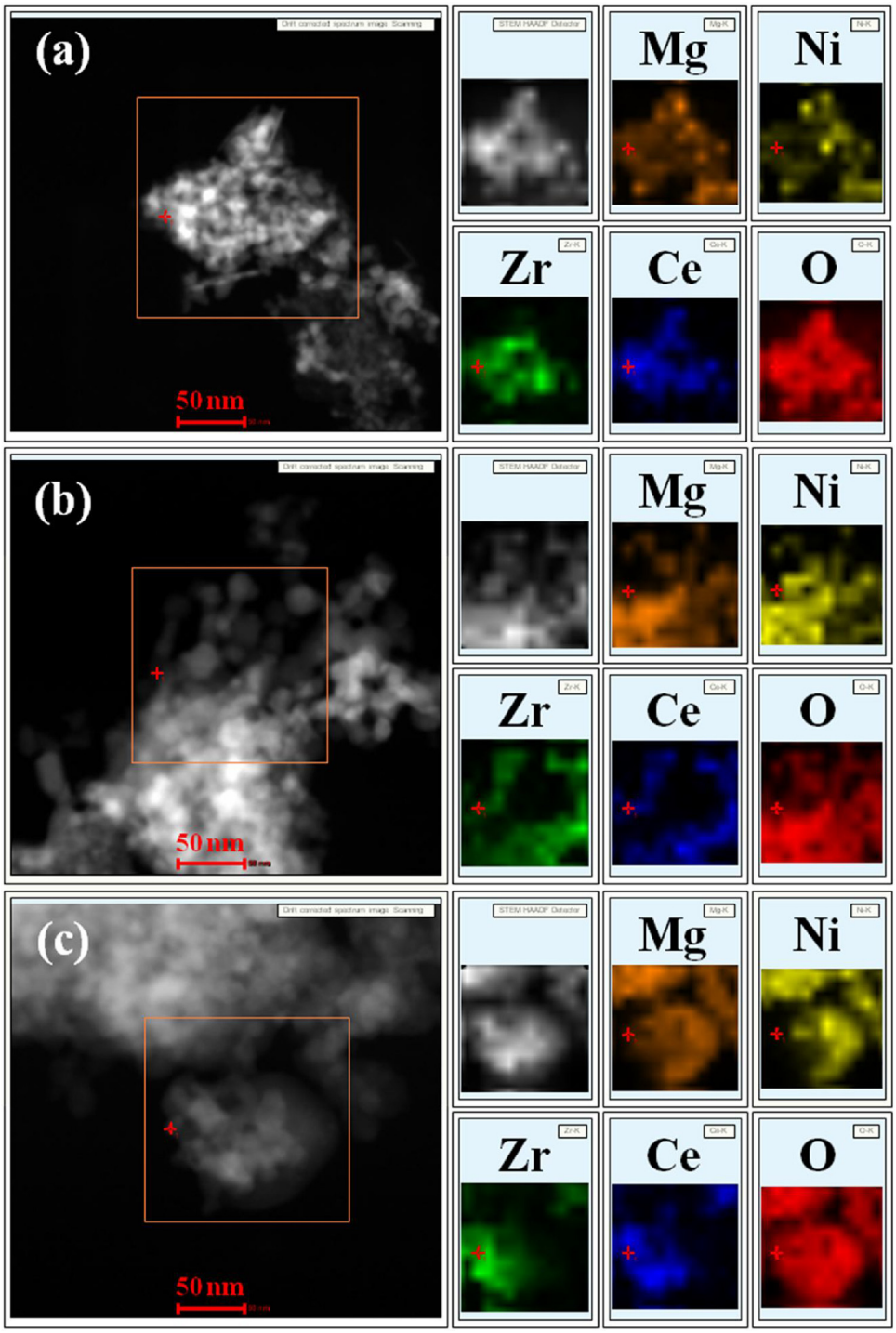

Fig. 5. TEM elemental mapping results of (a) Ni-MgO-$Ce_{0.8}Zr_{0.2}O_2$ (Co-precipitation), (b) Ni-MgO/$Ce_{0.8}Zr_{0.2}O_2$ (Co-impregnation), (c)Ni/MgO/$Ce_{0.8}Zr_{0.2}O_2$ (Sequential impregnation). Adapted from Ref. [119]. Copyright 2013 Elsevier.

the DRM reaction. The SMSI is formed by the presence of homogeneous solid solution such as $RhMg_2O_4$, NiO-MgO, $NiAl_2O_4$, $MgAl_2O_4$, $LaNiO_3$ and $LaSrCoO_3$. Homogeneous solid solution formed by strong interaction between catalyst components helps to incorporate the active metals into supports or promoters, resulting in the high dispersion and small size of active metals. Therefore, this property offers the excellent catalytic activity as well as the resistance against sintering and carbon formation. In particular, this property is much more important in the DRM reaction because of the high reaction temperature of DRM ($> 750\,^{\circ}C$) and larger carbon source compared to the conventional reforming reaction. Several literatures demonstrate that the catalysts having the SMSI have high metal surface area, high metal dispersion and small metal size, which are key properties for the catalytic application of DRM. However, forming the solid solution between components is determined by the kind of metal, support and promoter. When the catalyst is designed, the combination of the components should be considered. Metal particles having no interaction with support or promoter are obviously prone to the deactivation. In addition to the SMSI, the metal particle size and metal dispersion are the property that directly affects the catalytic activity and stability. There are several ways to obtain the highly dispersed and small size metal catalyst such as strengthening the interaction, emerging with the noble metals or Co

Table 4
Comparison of the catalysts with reducibility in DRM.

Catalyst[a]	Reaction condition		Conversion (%)			Time on stream (h)	Characterization techniques	Remarks	Reference
	GHSV or Flow rate	Feed gas ratio	T (K)	CH_4	CO_2				
Ni, Al_2O_3, V, SG	700 $cm^3\ min^{-1}\ g_{cat}^{-1}$	CH_4:CO_2:N_2 1:1:5	898	60	–	9	H_2-chemisorption XRD, XPS	Doping V on Ni/Al_2O_3 avoids the formation of inactive Ni/Al_2O_4, resulting from the enhanced reducibility	[112]
Ni, Al_2O_3-ZrO_2, -, SG	11,160 ml $h^{-1}\ g_{cat}^{-1}$	CH_4:CO_2:N_2 2:2:1	1,073	83	92	50	TPR	The introduction of ZrO_2 avoids the formation of $NiAl_2O_4$, resulting from the enhanced reducibility	[113]
Ni, Al_2O_3, K, IMP	22,500 h^{-1}	CH_4:CO_2 1:1	973	57	68	24	TPR	The addition of K increases the reducibility of the Ni catalyst and suppress the coke formation.	[114]
Ni, Al_2O_3, K, SG/IMP	0.5 g h mol_{CH4}^{-1}	CH_4:CO_2 1:1	1,023	82	86	30	TPR	K modification on Ni catalyst increases the reducibility and it hinders the accumulation of carbon on the catalyst surface.	[115]
Ni, Al_2O_3, Pt, SEQ-IMP	0.4 g h mol^{-1}	CH_4:CO_2:O_2 2:2:1	1,123	96	47	–	None	The surface Pt atoms in bimetallic catalyst can enhance the catalyst reducibility via alloying and/or hydrogen spillover effect.	[116,117,118]
Ni, $Ce_{0.8}Zr_{0.2}O_2$, MgO, CP	480,000 h^{-1}	CH_4:CO_2:N_2 1:1:3	1,073	95	96	200	TPR	Co-precipitation method can uniformly disperse the catalyst composition thereby it has easier reducibility.	[119]

[a] Metal, Support, Promoter, Preparation method.

(Bimetal) or enhancing the reducibility of metal oxide. Since the conventional Ni catalysts have been demonstrated to be unsuitable at an industrial-scale of DMR, synthesizing the highly dispersed and small size metal catalyst with an excellent performance is prerequisite for success of process. Apart from the SMSI, dispersion and particle size, there are important properties for the DRM reaction such as basicity, oxygen storage capacity, reducibility, porosity and surface area, which are primarily in relation to the nature of support. Traditionally, the basicity of supports is one of key property for the steam or oxidative reforming reactions because the formation of carbon by the CH_4 decomposition is formed on the acid sites of supports. Using the basic supports for the DRM reaction have one more advantage that basic sites of catalysts accelerate the activation of mildly acidic CO_2, oxidizing the surface carbon. Likewise, the oxygen storage capacity of supports is one of important factor that contribute to the activation of CO_2, increasing the number of mobile oxygen on the catalyst surface. The mobile oxygen plays a role in eliminating the carbon formation by oxidizing C to CO. The basic nature and oxygen storage capacity are advantageous for preventing the carbon formation, but the high reaction temperature must be considered for designing the catalyst, which means that the supports of DRM catalysts should have a resistance to sintering such as MgO-promoted support, promoted reducible mixed oxides. On the other hand, the reducibility or reduction degree determine the number of active sites. Too strong interaction active metals and supports causes the poor reducibility or the formation of inactive phase, leading to the lack of active sites. These properties generally depend on the conditions of pre-reduction or pre-activation steps, the pre-treatment step at too high temperature could occur economic or technical problems. Thus, the reducibility of the catalysts having poor reducibility should be promoted by adding the noble metals or reducible supports. The catalysts with well-defined structures have great potential due to their high specific area, uniform and their interconnected porosity. The aim of this literature review was to provide appropriate directions for the dry reforming of methane on the catalyst, in order to establish the mature industrialization of this process in the future.

Acknowledgements

This work was supported by “Next Generation Carbon Upcycling Project” (Project No. 2017M1A2A2044372) through the National

Table 5
Comparison of the catalysts with porosity and surface area in DRM.

Catalyst[a]	Reaction condition		Conversion (%)			Time on stream (h)	Characterization techniques	Remarks	Reference
	GHSV or Flow rate	Feed gas ratio	T (K)	CH_4	CO_2				
Ni, MCM-41(SiO_2), Imp	50,000 mL $g_{cat}^{-1}\ h^{-1}$	CH_4:CO_2:He 1:1:2	1023	70	70	30	BET XRD TPR	The presence of a suitable amount of nickel in Ni-MCM-41 is beneficial for maintaining high catalytic activity and long-term stability	[120]
Ni, ZSM-5 (SiO_2-Al_2O_3), Imp	12,000 mL $g_{cat}^{-1}\ h^{-1}$	CH_4:CO_2 1:1	1073	95	98	30	FESEM	The ratio of Si/Al on Ni/ZSM-5 plays a crucial role in creating the well-crystallized structure of nano-sized catalysts	[121]
Ni, CaO, Al_2O_3, one-pot evaporation-induced self-assembly (EISA)	15,000 mL $g_{cat}^{-1}\ h^{-1}$	CH_4:CO_2 1:1	1073	79	77	50	Pore distribution TEM	The obtained mesoporous materials played a significant role in providing more accessible Ni active centers and stabilizing the Ni nanoparticles by the confinement effect.	[122]

[a] Metal, Support, Promoter, Preparation method.

Research Foundation (NRF) funded by the Ministry of Science and ICT, Republic of Korea.

References

[1] United Nations Framework Convention on Climate Change (UNFCCC), Adoption of the Paris Agreement, Report No. FCCC/CP/2015/L.9/Rev.1, (2015) http://unfccc.int/resource/docs/2015/cop21/eng/l09r01.pdf.
[2] J. Rogelj, M. den elzen, N. Höhne, T. Fransen, H. Fekete, H. Winkler, R. Schaeffer, F. Sha, K. Riahi, M. Meinshausen, Nature 534 (2016) 631–639.
[3] International Energy Agency (IEA), Energy Technology Perspectives 2017, (2017).
[4] P. Markewitz, W. Kuckshinrichs, W. Leitner, J. Linssen, P. Zapp, R. Bongartz, A. Schreiber, T.E. Müller, Energy Environ. Sci. 5 (2012) 7281–7305.
[5] S. Sokolov, E.V. Kondratenko, M.M. Pohl, A. Barkschat, U. Rodemerck, Appl. Catal. B: Environ. 113 – 114 (2012) 19–30.
[6] G.A. Olah, A. Goeppert, M. Czaun, G.K.S. Prakash, J. Am. Chem. Soc. 135 (135) (2013) 648–650.
[7] G.A. Olah, A. Goeppert, M. Czaun, T. Mathew, R.B. May, G.K.S. Prakash, J. Am. Chem. Soc. 137 (2015) 8720–8729.
[8] U. Izquierdo, V.L. Barrio, J. Requies, J.F. Cambra, M.B. Guemez, P.L. Arias, Int. J. Hydrogen Energy 38 (2013) 7623–7631.
[9] M. Yu, K. Zhu, Z. Liu, H. Xiao, W. Deng, X. Zhou, Appl. Catal. B: Environ. 148 – 149 (2014) 177–190.
[10] M. Yu, Y.A. Zhu, Y. Lu, G. Tong, K. Zhu, X. Zhou, Appl. Catal. B: Environ. 165 (165) (2015) 43–56.
[11] H. Wu, G. Pantaleo, V. La Parola, A.M. Venezia, X. Collard, C. Aprile, L.F. Liotta, Appl. Catal. B: Environ. 156 – 157 (2014) 350–361.
[12] A. Sternberg, C.M. Jens, A. Bardow, Green Chem. 19 (2017) 2244–2259.
[13] J.L. Ewbank, L. Kovarik, C.C. Kenvin, C. Sievers, Green Chem. 16 (2014) 885–896.
[14] T.D. Gould, A. Izar, A.W. Weimer, J.L. Falconer, J.W. Medlin, ACS Catal. 4 (2014) 2714–2717.
[15] X. Xie, T. Otremba, P. Littlewood, R. Schomäcker, A. Thomas, ACS Catal. 3 (2013) 224–229.
[16] D. Pakhare, J. Spivey, Chem. Soc. Rev. 43 (2014) 7813–7837.
[17] N.A.K. Aramouni, J.G. Touma, B.A. Tarboush, J. Zeaiter, M.N. Ahmad, Renew. Sustain. Energy Rev. 82 (2018) 2570–2585.
[18] O. Muraza, A. Galadima, Int. J. Energy Res. 39 (2015) 1196–1216.
[19] S. Arora, R. Prasad, RSC Adv. 6 (2016) 108668–108688.
[20] P.M. Mortensen, I. Dybkjær, Appl. Catal. A Gen. 495 (2015) 141–151.
[21] M.C.J. Bradford, M.A. Vannice, Catal. Rev. – Sci. Eng. 41 (1999) 1–42.
[22] Y.H. Hu, E. Ruckenstein, Catal. Rev. – Sci. Eng. 44 (2002) 423–453.
[23] M.-S. Fan, A.Z. Abdullah, S. Bhatia, ChemCatChem 1 (2009) 192–208.
[24] J.-M. Lavoie, Front. Chem. 2 (2014) 1–17.
[25] N. Von der Assen, P. Voll, M. Peters, A. Bardow, Chem. Soc. Rev. 43 (2014) 7982–7994.
[26] M. Usman, W.M.A. Wan Daud, H.F. Abbas, Renew. Sustain. Energy Rev. 45 (2015) 710–744.
[27] M. Muraleedharan Nair, S. Kaliaguine, New J. Chem. 40 (2016) 4049–4060.
[28] B. Abdullah, N.A. Abd Ghani, D.-V.N. Vo, J. Clean. Prod. 162 (2017) 170–185.
[29] J. Lang, Z. Phys. Chem. 2 (1888) 161–183.
[30] F. Fischer, H. Tropsch, Brennstoff Chem 3 (1928) 39–46.
[31] R.E. Reitmeier, K. Atwood, H.A. Bennett, H.M. Baugh, Ind. Eng. Chem. 40 (1948) 620–626.
[32] J. Rostrup-Nielsen, US Patent 3791993 (1974).
[33] Intergovernmental Panel on Climate Change, IPCC First Assessment Report, (1990).
[34] D.A. Lashof, D.R. Ahuja, Nature 344 (1990) 529–531.
[35] W.D. Nordhaus, Science (80-) 258 (1992) 1315–1319.
[36] A.M. Gadalla, B. Bower, Chem. Eng. Sci. 43 (1988) 3049–3062.
[37] A.T. Ashcroft, A.K. Cheetham, M.L.H. Green, P.D.F. Vernon, Nature 352 (1991) 225–226.
[38] W.-J. Jang, D.-W. Jeong, J.-O. Shim, H.-M. Kim, H.-S. Roh, I.H. Son, S.J. Lee, Appl. Energy 173 (2016) 80–91.
[39] S. Wang, G.Q. Lu, G.J. Millar, Energy Fuels 10 (1996) 896–904.
[40] J. Zhang, H. Wang, A.K. Dalai, J. Catal. 249 (2007) 300–310.
[41] M.K. Nikoo, N.A.S. Amin, Fuel Process. Technol. 92 (2011) 678–691.
[42] J.R. Rostrup-Nielsen, J.H. Bak Hansen, J. Catal. 144 (1993) 38–49.
[43] J.T. Richardson, M. Garrait, J.K. Hung, Appl. Catal. A Gen. 255 (2003) 69–82.
[44] P. Ferreira-Aparicio, I. Rodríguez-Ramos, J.A. Anderson, A. Guerrero-Ruiz, Appl. Catal. A Gen. 202 (2000) 183–196.
[45] F. Menegazzo, M. Signoretto, F. Pinna, P. Canton, N. Pernicone, Appl. Catal. A Gen. 439–440 (2012) 80–87.
[46] H.Y. Wang, E. Ruckenstein, Appl. Catal. A Gen. 204 (2000) 143–152.
[47] E. Ruckenstein, Y.H. Hu, Appl. Catal. A Gen. 133 (1995) 149–161.
[48] E. Ruckenstein, Y.H. Hu, J. Catal. 162 (1996) 230–238.
[49] E. Ruckenstein, Y.H. Hu, Appl. Catal. A Gen. 154 (1997) 185–205.
[50] Y.H. Hu, E. Ruckenstein, Catal. Lett. 43 (1997) 71–77.
[51] E. Ruckenstein, Y.H. Hu, Catal. Lett. 51 (1998) 183–185.
[52] C. Batiot-Dupeyrat, F. Martinez-Ortega, M. Ganne, J.M. Tatibouët, Appl. Catal. A Gen. 206 (2001) 205–215.
[53] C. Batiot-Dupeyrat, G. Valderrama, A. Meneses, F. Martinez, J. Barrault, J.M. Tatibouët, Appl. Catal. A Gen. 248 (2003) 143–151.
[54] C. Batiot-Dupeyrat, G.A.S. Gallego, F. Mondragon, J. Barrault, J.M. Tatibouët, Catal. Today 107–108 (2005) 474–480.
[55] G. Valderrama, A. Kiennemann, M.R. Goldwasser, Catal. Today 113–135 (2008) 142–148.
[56] G. Valderrama, A. Kiennemann, M.R. Goldwasser, J. Power Sources 195 (2010) 1765–1777.
[57] G. Valderrama, C. Urbina De Navarro, M.R. Goldwasser, J. Power Sources 234 (2013) 31–37.
[58] S.M. Lima, J.M. Assaf, M.A. Peña, J.L.G. Fierro, Appl. Catal. A Gen. 311 (2006) 94–104.
[59] B. de Caprariis, P. de Filippis, V. Palma, A. Petrullo, A. Ricca, C. Ruocco, M. Scarsella, Appl. Catal. A Gen. 517 (2016) 47–55.
[60] N. Sahli, C. petit, A.C. Roger, A. Kiennemann, S. Libs, M.M. Bettahar, Catal. Today 113 (2006) 187–193.
[61] J. Guo, H. Lou, H. Zhao, D. Chai, X. Zheng, Appl. Catal. A Gen. 273 (2004) 75–82.
[62] J. Zhang, H. Wang, A.K. Dalai, Appl. Catal. A Gen. 339 (2008) 121–129.
[63] W.-J. Jang, D.-W. Jeong, J.-O. Shim, H.-M. Kim, W.-B. Han, J.W. Bae, H.-S. Roh, Renew. Energy 79 (2015) 91–95.
[64] W.-J. Jang, D.-W. Jeong, J.-O. Shim, H.-S. Roh, I.H. Son, S.J. Lee, Int. J. Hydrogen Energy 38 (2013) 4508–4512.
[65] J. Wei, E. Iglesia, J. Catal. 224 (2004) 370–383.
[66] J. Wei, E. Iglesia, Angew. Chem. Int. Ed. 43 (2004) 3685–3688.
[67] J. Wei, E. Iglesia, J. Phys. Chem. B 108 (2004) 4094–4103.
[68] J. Wei, E. Iglesia, Phys. Chem. Chem. Phys. 6 (2004) 3754–3759.
[69] J. Wei, E. Iglesia, J. Catal. 225 (2004) 116–127.
[70] J. Wei, E. Iglesia, J. Phys. Chem. B 108 (2004) 7253–7262.
[71] S. Wang, G.Q. Lu, Appl. Catal. B: Environ. 19 (1998) 267–277.
[72] G. Xu, K. Shi, Y. Gao, H. Xu, Y. Wei, J. Mol. Catal. A: Chem. 137 (1999) 47–54.
[73] I.G.O. Črnivec, P. Djinović, B. Erjavec, A. Pintar, Chem. Eng. J. 207–208 (2012) 299–307.
[74] L. Xu, H. Song, L. Chou, Appl. Catal. B: Environ. 108–109 (2011) 177–190.
[75] J.-E. Min, Y.-J. Lee, H.-G. Park, C. Zhang, K.-W. Jun, J. Ind. Eng. Chem. 26 (2015) 375–383.
[76] N. Habibi, Y. Wang, H. Arandiyan, M. Rezaei, ChemCatChem 8 (2016) 3600–3610.
[77] N. Habibi, Y. Wang, H. Arandiyan, M. Rezaei, Int. J. Hydrogen Energy 42 (2017) 24159–24168.
[78] F.R. Shamskar, F. Meshkani, M. Rezaei, J. CO2 Util. 22 (2017) 124–134.
[79] E. Akbari, S.M. Alavi, M. Rezaei, Fuel 194 (2017) 171–179.
[80] E. Akbari, S.M. Alavi, M. Rezaei, J. CO2 Util. 24 (2018) 128–138.
[81] N. Rahemi, M. Haghighi, A.A. BaBaluo, M.F. Jafari, P. Estifaee, J. Ind. Eng. Chem. 19 (2013) 1566–1576.
[82] W.-J. Jang, H.-M. Kim, J.-O. Shim, S.-Y. Yoo, K.-W. Jeon, H.-S. Na, Y.-L. Lee, D.-W. Jeong, J.W. Bae, I.W. Nah, H.-S. Roh, Green Chem. (2013), https://doi.org/10.1039/c7gc03605a in press.
[83] Z.Y. Hou, P. Chen, H.L. Fang, X.M. Zheng, T. Yashima, Int. J. Hydrogen Energy 31 (2006) 555–561.
[84] C. Carrara, J. Munera, E.A. Lombardo, L.M. Cornaglia, Top. Catal. 51 (2008) 98–106.
[85] P. Chen, H.B. Zhang, G.D. Lin, K.R. Tsai, Appl. Catal. A Gen. 166 (1998) 343–350.
[86] K. Fujimoto, K. Omata, T. Nozaki, O. Yamazaki, Y. Han, Energy Convers. Manage. 33 (1992) 529–536.
[87] S.-E. Park, J.-S. Chang, H.-S. Roh, M. Anpo, H. Yamashita, Stud. Surf. Sci. Catal. 114 (1998) 395–398.
[88] J.-S. Chang, S.-E. Park, H. Chon, Appl. Catal. A Gen. 145 (1996) 111–124.
[89] V.R. Choudhary, B.S. Uphade, A.S. Mamman, Catal. Lett. 32 (1995) 387–390.
[90] V.R. Choudhary, A.M. Rajput, Ind. Eng. Chem. Res. 35 (1996) 3934–3939.
[91] J.A.C. Dias, J.M. Assaf, Catal. Today 85 (2003) 59–68.
[92] S. Sengupta, G. Deo, J. CO_2 Util. 10 (2015) 67–77.
[93] F. Solymosi, G. Kutsan, A. Erdohelyi, Catal. Lett. 11 (1991) 149–156.
[94] P. Djinovic, J. Batista, A. Pintar, Int. J. Hydrogen Energy 37 (2012) 2699–2707.
[95] J.H. Bitter, K. Seshan, J.A. Lercher, J. Catal. 171 (1997) 279–286.
[96] J.H. Bitter, K. Seshan, J.A. Lercher, Top. Catal. 10 (2000) 295–305.
[97] K. Nagaoka, K. Seshan, J.A. Lercher, K. Aika, Catal. Lett. 70 (2000) 109–116.
[98] K. Nagaoka, K. Seshan, J.A. Lercher, K. Aika, Stud. Surf. Sci. Catal. 136 (2001) 129–136.
[99] X. Li, J.-S. Chang, S.-E. Park, Chem. Lett. 28 (1999) 1099–1100.
[100] H.-S. Roh, K.-W. Jun, W.-S. Dong, S.-E. Park, Y.-S. Baek, Catal. Lett. 74 (2001) 31–36.
[101] H.-S. Roh, W.-S. Dong, K.-W. Jun, S.-E. Park, Chem. Lett. 1 (2001) 88–89.
[102] H.-S. Roh, K.-W. Jun, S.-C. Baek, S.-E. Park, Chem. Lett. 10 (2001) 1048–1049.
[103] W.-S. Dong, K.-W. Jun, H.-S. Roh, Z.-W. Liu, S.-E. Park, Catal. Lett. 78 (2002) 215–222.
[104] H.-S. Roh, K.-W. Jun, W.-S. Dong, J.-S. Chang, S.-E. Park, Y.-I. Joe, J. Mol. Catal. A: Chem. 181 (2002) 137–142.
[105] W.-S. Dong, H.-S. Roh, K.-W. Jun, S.-E. Park, Y.-S. Oh, Appl. Catal. A Gen. 226 (2002) 63–72.
[106] H.S. Potdar, H.-S. Roh, K.-W. Jun, M. Ji, Z.-W. Liu, Catal. Lett. 84 (2002) 95–100.
[107] H.-S. Roh, K.-W. Jun, S.-E. Park, Appl. Catal. A Gen. 251 (2003) 275–283.
[108] H.-S. Roh, H.S. Potdar, K.-W. Jun, Catal. Today 93 – 95 (2004) 39–44.
[109] H.-S. Roh, H.S. Potdar, K.-W. Jun, J.-W. Kim, Y.-S. Oh, Appl. Catal. A Gen. 276 (2004) 231–239.
[110] F. Wang, L. Xu, J. Yang, J. Zhang, L. Zhang, H. Li, Y. Zhao, H.X. Li, K. Wu, G.Q. Xu, W. Chen, Catal. Today 281 (2017) 295–303.
[111] J. Zhu, X. Peng, L. Yao, X. Deng, H. Dong, D. Tong, C. Hu, Int. J. Hydrogen Energy 38 (2013) 117–126.
[112] A. Valentini, N.L.V. Carreno, L.F.D. Probst, P.N. Lisboa-Filho, W.H. Schreiner, E.R. Leite, E. Lingo, Appl. Catal. A Gen. 255 (2003) 211–220.
[113] H. Li, J. Wang, Chem. Eng. Sci. 59 (2004) 4861–4867.

[114] J. Juan-Juan, M.C. Roman-Martinez, M.J. Illan-Gomez, Appl. Catal. A Gen. 301 (2006) 9–15.
[115] A.E.C. Luna, M.E. Iriarte, Appl. Catal. A Gen. 343 (2008) 10–15.
[116] O. Yamazaki, K. Tomishige, K. Fujimoto, Appl. Catal. A Gen. 136 (1996) 49–56.
[117] K. Tomishige, S. Kanazawa, M. Sato, K. Ikushima, K. Kunimori, Catal. Lett. 84 (2002) 69–74.
[118] M. Nurunnabi, B. Li, K. Kunimori, K. Suzuki, K.I. Fujimoto, K. Tomishige, Appl. Catal. A Gen. 292 (2005) 272–280.
[119] D.-W. Jeong, W.-J. Jang, J.-O. Shim, H.-S. Roh, I.H. Son, S.J. Lee, Int. J. Hydrogen Energy 38 (2013) 13649–13654.
[120] D. Liu, Raymond Lau, A. Borgna, Y. Yang, Appl. Catal. A Gen. 258 (2009) 110–118.
[121] G. Moradi, F. khezeli, H. Hemmati, J. Nat. Gas Sci. Eng. 33 (2016) 657–665.
[122] L. Xu, H. Song, L. Chou, ACS Catal. 2 (2012) 1331–1342.